Structural Change of 1-Butyl-3-methylimidazolium Tetrafluoroborate + Water Mixtures Studied by Infrared Vibrational Spectroscopy

ARTICLE *in* THE JOURNAL OF PHYSICAL CHEMISTRY B · FEBRUARY 2008

Impact Factor: 3.3 · DOI: 10.1021/jp0746650 · Source: PubMed

8 AUTHORS, INCLUDING:

Doseok Kim
Sogang University
122 PUBLICATIONS **2,131** CITATIONS

SEE PROFILE

Structural Change of 1-Butyl-3-methylimidazolium Tetrafluoroborate + Water Mixtures Studied by Infrared Vibrational Spectroscopy

Yoonnam Jeon,[†] Jaeho Sung,[†] Doseok Kim,*[,†] Chungwon Seo,[‡] Hyeonsik Cheong,[‡] Yukio Ouchi,[§] Ryosuke Ozawa,[||] and Hiro-o Hamaguchi[||]

Department of Physics and Interdisciplinary Program of Integrated Biotechnology, Sogang University, Seoul 121-742 Korea, Department of Physics, Sogang University, Seoul 121-742 Korea, Department of Chemistry, Nagoya University, Chikusa-ku, Nagoya 464-8602 Japan, and Department of Chemistry, The University of Tokyo, Tokyo, 113-0033, Japan

Received: June 15, 2007; In Final Form: October 31, 2007

Mixtures of ionic liquid (IL, 1-butyl-3-methylimidazolium tetrafluoroborate, [BMIM][BF_4]) and water with varying concentrations were studied by attenuated total reflection infrared absorption and Raman spectroscopy. Changes in the peak intensities and peak positions of CH_x ($x = 1, 2, 3$) vibration modes of the cation of the IL and OH vibration modes of the water molecules were investigated. Peaks from normal-mode stretch vibrations of CH bonds belonging to the imidazolium ring of the cation did not change their positions, while those from the terminal methyl group of the butyl chain blueshifted by ∼10 cm^{-1} with the addition of water. On the other hand, change in the spectral shape in the OH stretch vibration region shows hydrogen-bonding network of water molecules breaking down rapidly as the IL is added. Trends in the change of the peak positions and the peak intensities suggested qualitative change of the intermolecular structure in the [BMIM][BF_4] + H_2O mixture at 32 ± 2 and 45 ± 2 mol/L of water concentration.

1. Introduction

Room-temperature ionic liquids (ILs) are salts made of organic cations and anions and are in liquid phase at room temperature.[1,2] Since these ILs are nonvolatile, nonflammable, and a good solvent for many chemicals, they are gaining interest as environment-friendly solvents for a range of chemical processes[3−5] or as important constituents for possible applications in electrochemistry.[6,7] As they only consist of ions, ILs are known as very strong hygroscopic material, and even a small amount of added water is known to induce a change of ILs properties by interaction with ILs.[8] Thus there have been several reports that studied the IL + water system recently.[9−12]

The structural change of water in a solution of ionic salts is also an interesting issue, both fundamentally and practically. Broad, overlapping OH peaks in the spectrum of bulk water are known to change with temperature and pressure.[13−15] Addition of solute molecules like inorganic salt or organic materials also changed its spectral shape, from which the change in the intermolecular structure has been inferred.[16−20] Aqueous salt solution in particular is a system of environmental interest as uptake of halide anions from a seawater system is considered a main cause of ozone depletion by oxidation processes.[17,21] However the spectral changes observed in an aqueous inorganic salt solution have been rather small, mainly due to the solubility limit of the most inorganic salts.[16,17] By contrast, many ILs are soluble in water in the whole solubility range[22−24] but have just small overlapping spectral features at the shoulder (2800−3200 cm^{-1}) of the OH spectral range (3000−3800 cm^{-1}). Therefore an IL is an ideal system to study the structural change of water due to anions and cations.

In this report, we chose 1-butyl-3-methylimidazolium tetrafluoroborate ([BMIM][BF_4]) mixed with water for spectroscopic investigation in the infrared range. [BMIM][BF_4] is ideally suited as it is one of the most popular ILs and miscible with water throughout the entire range of bulk mole fraction. We obtained the attenuated total reflection infrared (ATR-IR) absorption spectra at several concentrations and determined the CH and OH band positions and intensities for all concentrations. The fitted data allowed us to propose structural organizations of [BMIM][BF_4] + H_2O system with concentration changes since several features such as peak position of CH vibrational mode and the relative area of OH vibrational modes showed discontinuous changes with concentration. The low-frequency modes of the cation and anion of the IL observed with Raman spectroscopy showed similar trends as those observed in ATR-IR.

2. Experiment

[BMIM][BF_4] (purity better than 99%, water contents < 350 ppm, chloride content < 20 ppm) was purchased from C-TRI in Korea and used without further purification. Figure 1 shows the structure of $[BMIM]^+[BF_4]^-$. H_2O was doubly distilled, and D_2O was purchased from Aldrich. HDO solution (5 mol %) was made by mixing H_2O and D_2O with a volumetric ratio of 1:1.[25,26]

ATR (SensIR DuraSample/RII) measurements were made at room temperature. IR absorbance spectrum of IL/water mixture was taken from 650 to 4000 cm^{-1} with 4-cm^{-1} resolution and averaged 10 times. Wiping off the sample from the ATR prism (prism made of diamond) surface with kimwipes eliminated all

* To whom correspondence should be addressed. Fax: +82-2-711-4518. E-mail: doseok@sogang.ac.kr.
[†] Department of Physics and Interdisciplinary Program of Integrated Biotechnology, Sogang University.
[‡] Department of Physics, Sogang University.
[§] Nagoya University.
[||] The University of Tokyo.

10.1021/jp0746650 CCC: $40.75
Published on Web 01/03/2008

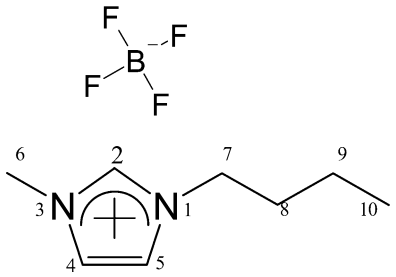

Figure 1. Chemical structure of [BMIM][BF_4].

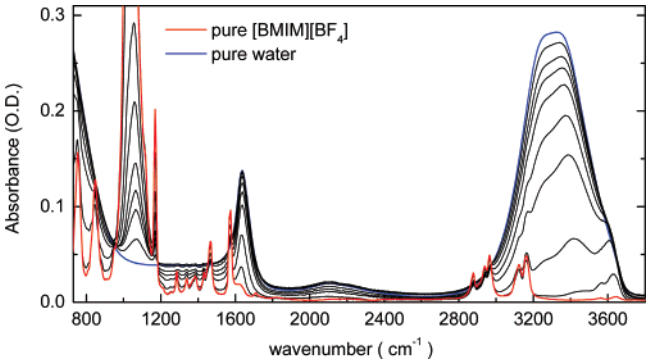

Figure 2. ATR absorption spectra of [BMIM][BF_4] + H_2O mixtures in the 650−4000-cm^{-1} range. The solid red line represents the absorption spectrum of pure [BMIM][BF_4], and the solid blue line represents the absorption spectrum of the pure water. The lines in between are the absorption spectra for the 53, 48, 46, 44, 38, 30, 14, and 4.3 mol/L water concentrations.

the absorption features from the spectrum, indicating that there were no adsorbed molecules or sample residue on the surface. To make sure, the prism surface was cleaned with methanol whenever the sample was changed. The Raman spectrum was taken in the quasi-backscattering geometry using 50 mW of the 514.5-nm line of an Ar ion laser as the excitation source focused to a line of 5 mm × 100 μm. The scattered light was filtered with a holographic edge filter and dispersed by a Spex 0.55-m spectrometer and detected with a liquid-nitrogen-cooled back-illuminated charge-coupled device (CCD) detector array. Both the spectral resolution and the accuracy in the Raman shift are estimated to be approximately 2 cm^{-1}. Each spectrum was averaged 10 times, and all measurements were done at room temperature.

3. Results and Discussion

Band Fitting and Peak Assignments. Figure 2 shows the ATR-IR absorption spectra of aqueous [BMIM][BF_4] at different concentrations. The pure water[25] and pure [BMIM][BF_4][27,28] spectrum in this range have been studied, and the peaks were assigned in previous reports. In this study, we concentrated on the CH_x and OH stretch vibrations regions above 2800 cm^{-1} as they are representative of structural changes in water and in $[BMIM]^+$ cation. Figure 3 is the close up of Figure 2 in the OH-stretch band, and Figure 4 shows the CH_x (x = 1, 2, 3) vibration mode peaks of [BMIM][BF_4] in the range of 2800−3200 cm^{-1}. As the absorption spectra of the CH_x vibration mode overlapped with OH vibration modes,[8,26] we also measured ATR-IR spectra from [BMIM][BF_4] + D_2O mixtures. In light and heavy water, simulation by Gaussian band fitting gave similar results for the CH band positions and intensities. Additionally, [BMIM][BF_4] + HDO mixture was prepared by isotopic substitution, from which the OH peaks in the weakly bonded environment were assigned.

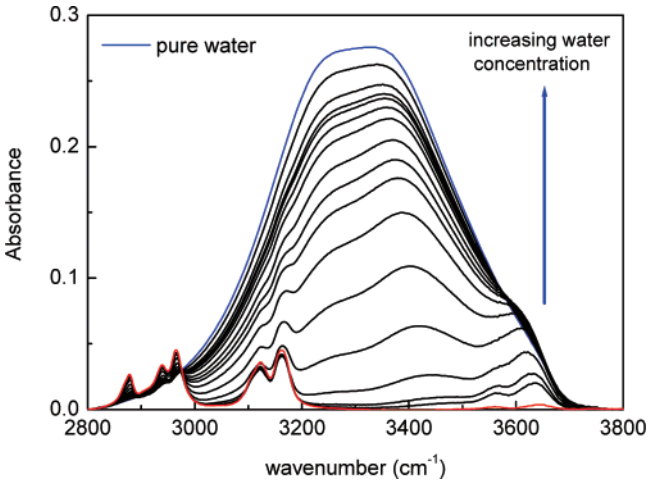

Figure 3. ATR absorption spectra of [BMIM][BF_4] + H_2O mixtures in the 2800−3800-cm^{-1} range. The bottom-most red line represents the absorption spectrum of pure [BMIM][BF_4], and the topmost blue line represents the absorption spectrum of the pure water. The lines in between are the absorption spectra for the 53, 48, 46, 44, 41, 38, 30, 23, 14, 7.9, 4.3, and 2.6 mol/L water concentrations.

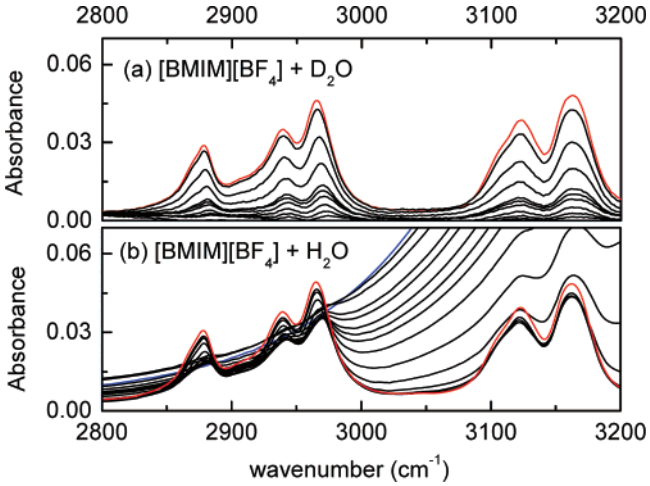

Figure 4. (a) The ATR absorption spectra in the range of 2800−3200 cm^{-1} for the [BMIM][BF_4] + D_2O mixture with varying the D_2O concentration. The lines are the absorption spectra for the 54, 53, 49, 46, 44, 41, 38, 35, 23, 14, and 2.6 mol/L D_2O concentrations, from bottom to top, and for pure [BMIM][BF_4] (the topmost red line). (b) ATR absorption spectra of [BMIM][BF_4] + H_2O mixtures (the same figure as in Figure 3) in the range of 2800−3200 cm^{-1} for comparison with panel a.

As shown in Figure 1, the cation is composed of a butyl chain and an imidazolium ring. The peak assignment of butyl chain is well known,[22,29−31] where five overlapped stretching mode peaks at ∼2866, ∼2876, ∼2915, ∼2938, and ∼2966 cm^{-1} were assigned to $\nu_{SS}CH_2$, $\nu_{SS}CH_3$, $\nu_{AS}CH_2$, $\nu_{FR}CH_3$, and $\nu_{AS}CH_3$, respectively (SS represents the symmetric stretch mode, AS represents the antisymmetric stretch mode, and FR stands for Fermi resonance).[22,31,32] Two peaks at ∼2998 cm^{-1} ($\nu_{SS}CH_3$) and ∼3063 cm^{-1} ($\nu_{AS}CH_3$) were assigned to the methyl group attached to the imidazolium core.[31−33] Finally, three peaks at ∼3114 cm^{-1} (νC(2)H), ∼3126 cm^{-1} (ν_{AS}HC(4)−C(5)H), and ∼3163 cm^{-1} (ν_{SS}HC(4)−C(5)H) were from the CH normal-mode vibrations of hydrogen attached directly to the imidazolium ring.[10,32,34]

As for the OH-spectral range of water molecule, the broad peak from 3000 to 3800 cm^{-1} of the bulk water represents inhomogeneous environment of water molecules due to hydrogen bonding. There have been different ways to fit this broad

TABLE 1: Gaussian Fitting Parameters for ATR Spectral Fits of OH Vibration[a]

	icelike[1]		liquidlike				weakly bonded (ss)[2]			weakly bonded (as)[3]		
water concentration (mol/L)	A_v	area	A_v	ω_v	σ_v	area	A_v	ω_v	area	A_v	ω_v	area
56	0.27	90	0.095	3455	132	22	0.027	3582	2.4	0.018	3639	0.95
50	0.22	78	0.094	3455	139	23	0.027	3585	2.4	0.017	3638	0.89
46	0.20	69	0.096	3453	143	24	0.029	3589	2.6	0.016	3639	0.86
41	0.17	52	0.096	3449	144	25	0.033	3592	2.9	0.016	3639	0.87
30	0.11	37	0.086	3450	143	22	0.039	3596	3.5	0.016	3640	0.86
24	0.068	24	0.071	3453	141	17	0.042	3600	3.8	0.016	3641	0.83
14	0.034	12	0.047	3461	135	11	0.040	3602	3.6	0.016	3641	0.87
7.9	0.012	4.5	0.022	3481	130	4.6	0.027	3602	2.5	0.018	3640	1.0
0							0.002	3564		0.004	3645	

[a] Fixed parameters: [1]ω_v 3275, σ_v 195; [2]σ_v 50; [3]σ_v 30.

OH band. The most prominent ones are around ~3270 and ~3450 cm^{-1}.[17,25,34] The former is often called the icelike peak as it is dominant when the water molecules form a well-ordered hydrogen-bonding network such as in ice, while the latter is called the liquidlike peak[10,14,35] as the relative enhancement of this peak is well-correlated with the more disordered structure of water (as in the case of temperature increase or addition of structure breaker in water).[13,14,36] We will follow the practice and will use these notations in this report.

In our [BMIM][BF_4] + water system (Figure 3), there is a clear shoulder consisting of two peaks at the high-frequency side of the usual OH peak.[8,16,37] As they are at the high-frequency side of the liquidlike peak, the hydrogen bonding of these molecules should be even weaker. Welton and co-workers assigned these peaks as symmetric (ν_1 at 3560 cm^{-1}) and antisymmetric (ν_3 at 3640 cm^{-1}) stretch normal-mode vibrations of H_2O molecule hydrogen bonded on each side by the anion.[8] When a small amount of HDO was used in a mixture instead of H_2O, it showed only single peak around the midpoint at ~3600 cm^{-1}, confirming the above assignment.[8]

As can be seen in Figure 4a for [BMIM][BF_4] + D_2O mixtures, an antisymmetric HC(4)−C(5)H stretching mode (ν_{AS}HC(4)−C(5)H) peak at ~3126 cm^{-1} and a symmetric HC(4)−C(5)H stretching mode (ν_{SS}HC(4)−C(5)H) peak at ~3163 cm^{-1} of imidazolium ring did not change with concentration and thus held fixed in the fitting. However, the peaks originating from the butyl chain showed measurable blueshift, as is known for the other cases of aqueous solutions. These fitting parameters deduced from the spectra of [BMIM][BF_4] + D_2O mixtures were held fixed in fitting the OH range spectra for [BMIM][BF_4] + H_2O mixtures. For the fitting in the OH range, Brooksby et al. demonstrated the ambiguity of fitting the water spectrum by showing very different sets of fitting parameters could fit the same water spectrum equally well.[38] Thus care should be taken in quantitative analysis of the peak intensities in the OH region. Therefore, we used the Gaussian parameters of the previous works to fit our spectra.[17,39] Table 1 represents the Gaussian fitting parameters used to fit the ATR spectra. A_v represents the peak amplitude, ω_v represents the peak position, and $\sqrt{2}\sigma_v$ represents the full-width at half-maximum of the vth vibration mode. In the fitting of the OH spectra, the icelike water peak was fixed at ~3275 cm^{-1}, while the other peaks were allowed to change a little bit (20 cm^{-1} at most for the liquidlike OH peak, and ~5 cm^{-1} for weakly bonded OH peaks). The fitting values and area (integrated value between 2800 and 4000 cm^{-1}) for each concentration are shown in Table 1.[38]

The Raman spectra shows two bands at ~600 and 620 cm^{-1} for the gauche and trans conformation of the 1-butyl group, as has been assigned by Berg et al.[31] and Ozawa et al.[39] More specifically, they are considered to come from gauche and trans conformations around the C(7)−C(8) bonds in Figure 1. The peak around 765 cm^{-1} (shown in Figure 7b) is from stretching mode of the BF_4^- anion (νBF_4^-).[28] Above peaks from the Raman spectra were also fitted by Gaussian function, and the integrated area and the peak position for each concentration were used for quantitative analysis.

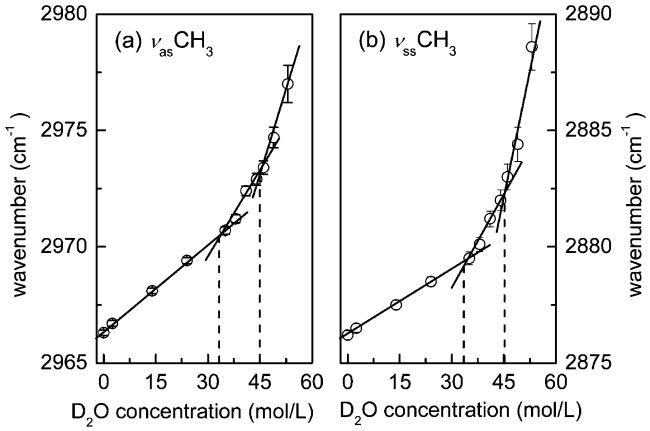

Figure 5. (a) Peak shift of $\nu_{AS}CH_3$, (b) peak shift of $\nu_{SS}CH_3$ with increasing the D_2O concentration in the [BMIM][BF_4] + D_2O mixture. Open circles represent the deconvoluted data from Figure 4a. Solid lines are the guide lines following the peak shift, and dashed lines indicate the concentration where the slope changes discontinuously.

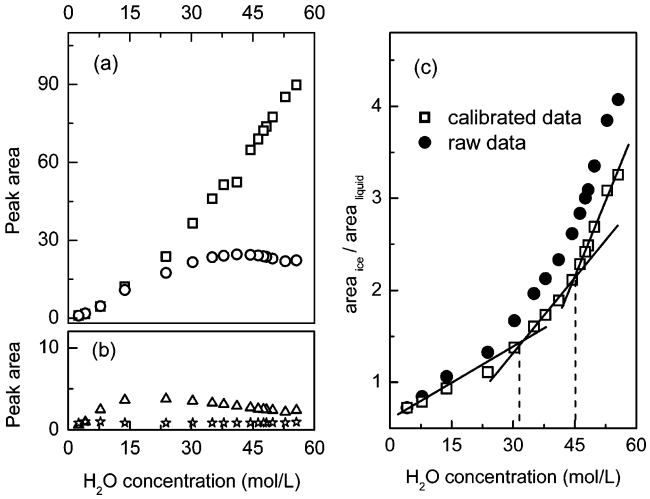

Figure 6. Peak areas of OH vibrational peaks of water molecule in the [BMIM][BF_4] + H_2O mixtures by Gaussian fitting with increasing water concentration. (a) Open squares and open circles represent the area of the icelike and liquidlike OH stretch mode peaks, respectively. (b) Open triangles and open stars represent the area of the symmetric and antisymmetric stretch mode of weakly bonded OH peak. (c) Ratios of the peak areas of the icelike and liquidlike peaks. Filled circles represent the raw data, and open square represent the ratios after the correction using eq 2. Solid lines are the guides to the eye, and dashed lines indicate the concentration where the slope changes discontinuously.

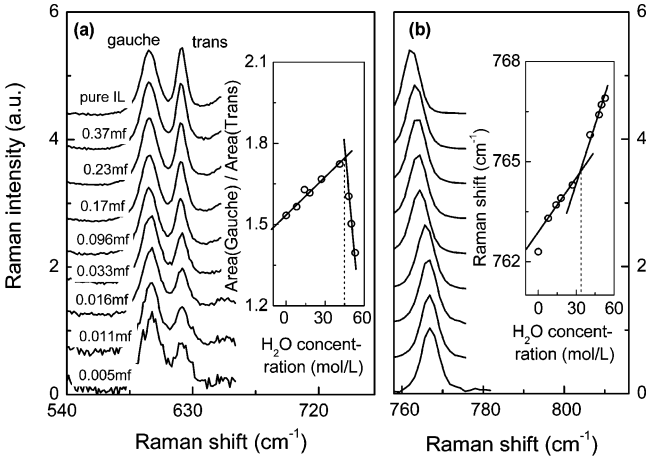

Figure 7. Normalized Raman data between 590 and 780 cm^{-1} with varying water concentrations. (a) The peaks at ~600 and 620 cm^{-1} are for gauche and trans forms of C(7)−C(8) in the butyl chain. In the inset, the open circle is the area ratio between the gauche and trans peaks with Gaussian fitting for each peak. Solid lines are the guide lines, and the dotted line is for the discontinuous point of the slope. (b) The peak around 765 cm^{-1} is from υBF_4^-, taken at the same concentrations as in panel a. In the inset, open circles are the peak shift from Gaussian fitting, solid lines are the guides to the eye, and the dotted line is for the discontinuous points of the slope.

Determination of the ATR-IR Band Intensities. Absorbance is a measure of light absorption in the medium and is proportional to the path length (d) as $A = \log(I_0/I) \propto d$.[40] In usual absorption measurements, the light is attenuated in transmission through a sample of known thickness, while in ATR geometry, the absorption takes place in the evanescent wave penetrating into the sample, which works to decrease the amplitude of internally reflected light. In this case, the effective path length (d_e) at each reflection is twice the penetration depth of the evanescent wave in ATR system as follows[41]

$$d_e = \frac{2}{k}(n_1\sqrt{\sin^2\theta - n_2^2/n_1^2})^{-1} \quad (1)$$

where k is the wavevector of the light for the vacuum, θ is the incident angle, n_1 is the refractive index of the prism (made of diamond), and n_2 is the refractive index of the sample. In our apparatus, $\theta = 45°$, and $n_1 = 2.38$ at 2.5−4.0 μm.[42]

Eq 1 shows that care needs to be taken in the quantitative analysis of the peak intensities as the change in the refractive index of the sample (e.g., caused by changing mixture concentrations) would alter the effective path length. For our samples, the refractive index of pure water is quite dispersive in the OH stretch range (1.12−1.49 at 25 °C),[43] while that of [BMIM]-[BF_4] is ~1.37 (at 20 °C)[44] at the frequency range under investigation. For the [BMIM][BF_4] + water mixture samples, the refractive index at each concentration was estimated by using the effective medium theory.[45] For example, in comparing the peak intensities of icelike and liquidlike peaks in Figure 6c, the refractive index at each peak position of pure samples was used to deduce the refractive index of the mixture of specific composition. The area ratio of (icelike OH peak)/(liquidlike OH peak) in our experimental condition is proportional to

$$n_{liq}\sqrt{n_1^2 - 2n_{ice}^2}/n_{ice}\sqrt{n_1^2 - 2n_{liq}^2} \quad (2)$$

where n_{ice} and n_{liq} are the refractive indices of the mixture at the corresponding peak positions. The ratio values after the correction using eq 2 were shown together with those from the raw data for comparison in Figure 6c.

In case of a mixture we should know the total volume of the mixture to get the number density of each ingredient. The total volume of the [BMIM][BF_4] + H_2O mixture was found to increase slightly as compared to the sum of the volumes of [BMIM][BF_4] and water.[24] That is $V = V_{id} + V_{ex}$, where V_{id} is the ideal molar volume of the mixtures, and V_{ex} is the excess molar volume ($cm^3\ mol^{-1}$) with $V_{ex} > 0$ in our case. Following ref 24 and neglecting the small difference in temperature, we estimated (shown in Table 2) the relation between the mole fraction of the mixture and the number density of each constituent.

CH_x Stretch Vibration. Figure 3 represents the ATR absorption spectra of the [BMIM][BF_4] + H_2O solution with varying water concentrations; the red line at the bottom represents the absorption spectrum of pure [BMIM][BF_4], and the topmost blue line represents the absorption spectrum of pure water. The features between 3000 and 3200 cm^{-1} are the C(2)H vibration mode peak and the HC(4)−C(5)H vibration mode peaks of the imidazolium ring, and overlapped peaks between the 2800 and 3000 cm^{-1} are due to CH_2 and CH_3 vibrations of the butyl chain in the cation. ATR spectra from [BMIM][BF_4] + D_2O used to better deduce the CH_x peak positions and intensities are compared with those from [BMIM][BF_4]+H_2O in parts a and b of Figure 4.

Parts a and b of Figure 5 show the peak shifts of $\nu_{AS}CH_3$ and $\nu_{SS}CH_3$ deduced from fitting Figure 4a. Solid lines in each graph are guides to the eye for the peak shift vs D_2O concentration. When organic molecules are mixed with water, the slight blueshift of CH_3 peak positions with the addition of water was reported previously.[19,46−49] Mizuno et al. studied this aqueous mixture system with NMR and proposed that the CH···O interaction would be weak repulsion between the electron of hydrogen and negative charge of oxygen atom.[48] We analyzed our spectra with multipeak Gaussian to extract the exact peak positions at different concentrations. We mainly relied on Figure 4a with [BMIM][BF_4] + D_2O mixture as it is less affected by the shoulder of OH stretches, but Figure 4b also gave comparable values for peaks shift vs concentrations. The peak shift thus obtained (shown in parts a and b of Figure 5) was ~10 cm^{-1} to the blue for $\nu_{AS}CH_3$ and $\nu_{SS}CH_3$ with the increase of D_2O concentration.[50] It should be reminded that the CH peaks belonging to the imidazolium core hardly shifted with the addition of water. As the BF_4^- anion should be strongly bound to the imidazolium cation for pure [BMIM][BF_4], one can suggest that they are still strongly attached even when [BMIM]-[BF_4] is diluted. On the other hand, a recent X-ray study reported that the anion−cation distance varied sensitively with even a small amount of added water,[51] and a conductivity study of ILs dissolved in several different solvents suggested that high dielectric constants of water facilitates the dissociation of anion and cation.[52] We propose that the BF_4^- anion would be bound to the imidazolium cation throughout the concentration range we investigated or that (in case they dissociate at high dilution) the electronic environment provided by the anion is similar to the water molecule as long as the interaction with the cation is concerned.

Furthermore, the slope of peak position vs concentration (Figure 5) is not constant but shown to change rather abruptly at 45 ± 2 mol/L of water number density (corresponding to 0.02 mole fraction of [BMIM][BF_4]) and 32 ± 2 mol/L of water number density (0.07 mole fraction of [BMIM][BF_4]). Dashed lines in parts a and b of Figure 5 indicate these points. As other spectroscopic quantities also showed discontinuous changes at

TABLE 2: Relation between the Concentration and the Mole Fraction of the Mixture

IL mole fraction	0.0	0.011	0.019	0.033	0.075	0.11	0.23	0.37	1.0
H_2O concentration (mol/L)	56	50	46	41	30	24	14	7.9	0
[BMIM][BF_4] concentration (mol/L)	0	0.56	0.90	1.4	2.5	3.1	4.0	4.6	5.4

these two concentrations, it could be suspected that qualitative changes in bulk structure take place at these mixture concentrations.

OH Stretch Vibration. ATR-IR absorption spectra in the OH-stretch region are shown in Figure 3. For pure water, the broad absorption can be fitted with two well-known peaks around 3270 and 3450 cm^{-1}.[14,53] With the addition of [BMIM][BF_4] to the water, the peak component at 3270 cm^{-1} quickly decreases and the whole absorption is shown to blueshift, indicating the hydrogen-bonding network of water is steadily disrupted. With the further increase in the IL concentration, the broad feature under 3500 cm^{-1} is further suppressed and two small peaks at higher frequency are shown to appear. They were assigned to symmetric (ν_1 at ~3657 cm^{-1}) and antisymmetric (ν_3 at ~3756 cm^{-1}) stretch normal-mode vibrations of H_2O molecule hydrogen bonded on each side by the anion.[8,16] This mixture system is unique as the absorption peaks from [BMIM][BF_4] are only at the shoulder of this OH stretch spectral feature, thus unambiguously showing continuous change of the bulk structure of water. The whole range of concentration could be fitted well with the above 4 peaks with only small change in the peak positions.

Figure 6a shows the changes in the area of the ice- and liquidlike peaks with the change of water concentration, and Figure 6b shows the peak areas of symmetric and antisymmetric stretch modes of weakly bonded OH obtained from the fitting. The icelike peak is indeed shown to decrease rapidly with the addition of [BMIM][BF_4], while liquidlike peak did not change appreciably until it dropped at very high concentration of IL. By dividing the icelike peak area at 3270 cm^{-1} by the liquidlike peak area at 3450 cm^{-1}, the changing number density of water molecules in the mixtures offsets in the numerator and the denominator, and this ratio can work qualitatively as an indicator of bulk water structure. As the refractive index changes with the change in the water concentration, the change in the penetration depth of the evanescent wave as in eq 1 should be accounted for in dealing with the mixture. In Figure 6c, open squares represent the area ratio (icelike/liquidlike) after the correction using eq 2, and they are shown to change a bit from the filled circles representing the ratio for the raw data. The ratio values in both data are shown to decrease rapidly with the increase in the [BMIM][BF_4] concentration, indicating the breakdown of the hydrogen-bonding network.[53] Upon close examination of Figure 6c, the slope is not constant but changes rather abruptly at ~45 and ~32 mol/L water concentrations, the same concentration values that showed the abrupt slope changes in parts a and b of Figure 5.

Raman Spectra. Figure 7 shows the Raman spectra from mixtures at several different concentrations. In Figure 7a showing the normalized Raman spectra for different mixtures, two peaks at ~ 600 and 620 cm^{-1} originated from the gauche and trans forms around C(7)−C(8) of the butyl chain (Figure 1). The inset of Figure 7a represents the area ratios between the gauche and trans forms. This ratio between the gauche and trans peaks increases and reaches a maximum at 45 ± 2 mol/L water concentration (0.02 mole fraction of [BMIM][BF_4]) and then decreases rapidly afterward. Thus some change in the butyl chain conformation could be inferred around this concentration. Figure 7b shows the normalized Raman peak from νBF_4^-, which blueshifts with increasing water concentration. As shown in the inset of Figure 7b, the peak shift of νBF_4^- is not linear, but the slope changes at around a 32 mol/L water concentration, the same concentration as in Figures 5 and 6c.

Structural Change of the Mixture. The spectral features obtained from fitting the spectra showed rather distinct changes at 32 ± 2 and 45 ± 2 mol/L. For examples from Figure 6c, the icelike peak is shown to grow more rapidly starting from ~32 mol/L. This is concurrent with the change in the peak-shift ratios in Figure 5a (terminal methyl group of the butyl chain in the cation) or Figure 7b (νBF_4^-). So it can be inferred that microscopic structure of water changed qualitatively, and that affected the interaction of water molecules with neighboring cations and anions as well. We propose the water molecules in the mixture began to form global hydrogen-bonding network around this concentration, and this structural change has an effect on the cations and anions.

The icelike peak is shown to grow even more rapidly (Figure 6) starting from ~45 mol/L. This also is the concentration where the peak-shift of terminal methyl group (parts a and b of Figure 5) and the trans−gauche ratio in Figure 7a change their varying trends. We proposed that $[BMIM]^+$ cations undergo structural change at this concentration, presumably by forming micelles or aggregates as the $[BMIM]^+$ concentration increases in the mixture. Surface tension measurements of [BMIM][BF_4] + H_2O showed abrupt change of surface tension at this concentration, and it was proposed as the critical micelle concentration[11] or onset of the change of surface structure,[22] which should affect the bulk structure of the mixture as well. The thermodynamic study of [BMIM][BF_4] + H_2O by Katayanagi et al. also reported change in the excess partial molar enthalpy near this concentration.[23] The change of slope in parts a and b of Figure 5 can be well explained by this idea as clustering of cations at this concentration would reduce the exposure of terminal methyl group with water, thus slowing down the methyl peak shift rate. Finally, the rather abrupt change in the trans−gauche ratio shown in Figure 7a would also be an indication of the structural change of the cation. It should be reminded that this trans−gauche ratio is a very sensitive indicator of bulk IL structure, as proposed by Hamaguchi and co-workers.[39]

5. Conclusion

[BMIM][BF_4] + H_2O mixtures at various concentrations were studied by ATR-IR and Raman spectroscopy. From the data fittings, we observed ~10 cm^{-1} blue shifts of $\nu_{SS}CH_3$ and $\nu_{AS}CH_3$ by increasing the H_2O concentration, even though ν_{AS}HC(4)−C(5)H and ν_{SS}HC(4)−C(5)H of the imidazolium ring did not show any peak shifts. Four overlapped bands were used to fit the spectra in the OH range between 3000 and 3800 cm^{-1}. The icelike water peak decreased rapidly with the addition of [BMIM][BF_4] in the mixtures. By comparison of the area ratio between the icelike and liquidlike water peaks, two discontinuous points of the slope were noticeable indicating the structural change of water structure. The low-frequency modes of the cation and anion of the IL observed with Raman spectroscopy showed similar trend as observed in ATR-IR. From these results, qualitative changes in the mixture structure at changes at 32 ± 2 and 45 ± 2 mol/L water concentration were proposed.

Acknowledgment. This work was supported by a Sogang University Research Grant in 2007. Y.O. acknowledges support from Grants-in-Aid for the Scientific Research in Priority Areas "Science of Ionic Liquids" from the Ministry of Education, Culture, Sports, Science and Technology of Japan and the Venture Business Laboratory Project "Advanced Nanoprocess Technologies" at Nagoya University.

References and Notes

(1) Seddon, K. R. *J. Chem. Tech. Biotechnol.* **1997**, *68*, 351.
(2) Welton, T. *Chem. Rev.* **1999**, *99*, 2071.
(3) Chauvin, Y.; Mussmann, L.; Olivier, H. *Angew. Chem., Int. Ed. Engl.* **1996**, *34*, 2698.
(4) Dyson, P. J.; Ellis, D. J.; Parker, D. G.; Welton, T. *Chem. Commun.* **1999**, *25*, 2418.
(5) Suarez, P. A. Z.; Dullius, J. E. L.; Einloft, S.; de Souza, R. F.; Dupont, J. *Inorg. Chim. Acta* **1997**, *255*, 207.
(6) Carlin, R. T.; De Long, H. C.; Fuller, J.; Trulove, P. C. *J. Electrochem. Soc.* **1994**, *141*, L73.
(7) Seki, S.; Ohno, Y.; Kobayashi, Y.; Miyashiro, H.; Usami, A.; Mita, Y.; Tokuda, H.; Watanabe, M.; Hayamizu, K.; Tsuzuki, S.; Hattori, M.; Terada, N. *J. Electrochem. Soc.* **2007**, *154*, A173.
(8) Cammarata, L.; Kazarian, S. G.; Salter, P. A.; Welton, T. *Phys. Chem. Chem. Phys.* **2001**, *3*, 5192.
(9) Hanke, C. G.; Lynden-Bell, R. M. *J. Phys. Chem. B* **2003**, *107*, 10873.
(10) Fitchett, B. D.; Conboy, J. C. *J. Chem. Phys. B* **2004**, *108*, 20255.
(11) Bowers, J.; Butts, C. P.; Martin, P. J.; Verqara-Gutierrez, M. C.; Heenan, R. K. *Langmuir* **2004**, *20*, 2191.
(12) Malham, I. B.; Letellier, P.; Turmine, M. *J. Phys. Chem. B* **2006**, *110*, 14212.
(13) Scherer, J. R.; Go, M. K.; Kint, S. *J. Phys. Chem.* **1974**, *78*, 1304.
(14) Raichlin, Y.; Millo, A.; Katzir, A. *Phys. Rev. Lett.* **2004**, *93*, 185703.
(15) Kawamoto, T.; Ochiai, S.; Kagi, H. *J. Chem. Phys.* **2004**, *120*, 5867.
(16) Walrafen, G. E. *J. Chem. Phys.* **1971**, *55*, 768.
(17) Liu, D.; Ma, G.; Levering, L. M.; Allen, H. C. *J. Phys. Chem. B* **2004**, *108*, 2252.
(18) Dillon, S. R.; Dougherty, R. C. *J. Phys. Chem. A* **2003**, *107*, 10217.
(19) D' Angelo, M.; Onori, G.; Santucci, A. *J. Chem. Phys.* **1994**, *100*, 3107.
(20) Scatena, L. F.; Brown, M. G.; Richmond, G. L. *Science* **2001**, *292*, 908.
(21) Ghosal, S.; Hemminger, J. C.; Bluhm, H.; Mun, B. S.; Hebenstreit, E. L. D.; Ketteler, G.; Ogletree, D. F.; Requejo, F. G.; Salmeron, M. *Science* **2005**, *307*, 563.
(22) Sung, J.; Jeon, Y.; Kim, D.; Iwahashi, T.; Iimori, T.; Seki, K.; Ouchi, Y. *Chem. Phys. Lett.* **2005**, *406*, 495.
(23) Katayanagi, H.; Nishikawa, K.; Shimozaki, H.; Miki, K.; Westh, P.; Koga, Y. *J. Phys. Chem. B* **2004**, *108*, 19451
(24) Seddon, K. R.; Stark, A.; Torres, M. J. *Pure Appl. Chem.* **2000**, *72*, 2275.
(25) Marechal, Y. *J. Chem. Phys.* **1991**, *95*, 5565.
(26) Wall, T. T.; Hornig, D. F. *J. Chem. Phys.* **1965**, *43*, 2079.
(27) Heimer, N. E.; Del Sesto, R. E.; Meng, Z.; Wilkes, J. S.; Carper, W. R. *J. Mol. Liq.* **2006**, *124*, 84.
(28) Katsyuba, S. A.; Zvereva, E. E.; Vidis, A.; Dyson, P. J. *J. Phys. Chem.* **2007**, *111*, 352.
(29) Li, Q.; Weng, S.; Wu, J.; Zhou, N. *J. Phys. Chem. B* **1998**, *102*, 3168.
(30) Brubach, J.-B.; Mermet, A.; Filabozzi, A.; Gerschel, A.; Lairez, D.; Krafft, M. P.; Roy, P. *J. Phys. Chem. B* **2001**, *105*, 430.
(31) Berg, R. W.; Deetlefs, M.; Seddon, K. R.; Shim, I.; Thompson, J. M. *J. Phys. Chem. B* **2005**, *109*, 19018
(32) Talaty, E. R.; Raja, S.; Storhaug, V. J.; Dölle, A.; Carper, W. R. *J. Phys. Chem. B* **2004**, *108*, 13177.
(33) Rivera−Rubero, S.; Baldelli, S. *J. Phys. Chem. B* **2006**, *110*, 4756.
(34) Carter, D. A.; Pemberton, J. E.; Woelfel, K. J. *J. Phys. Chem. B* **1998**, *102*, 9870.
(35) Chen, Y.; Zhang, Y.-H.; Zhao, L.-J. *Phys. Chem. Chem. Phys.* **2004**, *6*, 537.
(36) Ratcliffe, C. I.; Irish, D. E. *J. Phys. Chem.* **1982**, *86*, 4897.
(37) Eisenberg, D.; Kauzmann, W. *The structure and properties of water*; Oxford University; New York and Oxford, 1969.
(38) Brooksby, P. A.; Fawcett, W. R. *J. Phys. Chem. A* **2000**, *104*, 8307.
(39) Ozawa, R.; Hayashi, S.; Saha, S.; Kobayahi, A.; Hamaguchi, H. *Chem. Lett.* **2003**, *32*, 948.
(40) Sammon, C.; Mura, C.; Yarwood, J.; Everall, N.; Swart, R.; Hodge, D. *J. Phys. Chem. B* **1998**, *102*, 3402.
(41) Bertie, J. E.; Eysel, H. H. *Appl. Spectrosc.* **1985**, *39*, 392.
(42) Nikogosyan, D. N. *Properties of Optical and Laser-Related materials*; Wiley: New York, 1997.
(43) Bertie, J. E.; Lan, J. *Appl. Spectrosc.* **1996**, *50*, 1047.
(44) Iimori, T.; Iwahashi, T.; Ishii, H.; Seki, K.; Ouchi, Y.; Ozawa, R.; Hamaguchi, H.; Kim, D. *Chem. Phys. Lett.* **2004**, *389*, 321.
(45) Choy, T. C. *Effective Medium Theory*; Oxford: New York, 1999.
(46) Chang, H. C.; Jiang, J. C.; Tsai, W. C.; Chen, G. C.; Lin, S. H. *J. Phys. Chem. B* **2006**, *110*, 3302.
(47) Hobza, P.; Spirko, V.; Havlas, Z.; Buchhold, K.; Reimann, B.; Barth, H.; Brutschy, B. *Chem. Phys. Lett.* **1999**, *299*, 180.
(48) Mizuno, K.; Imafuji, S.; Ochi, T.; Ohta, T.; Maeda, S. *J. Phys. Chem. B* **2000**, *104*, 11001.
(49) Gu, Y.; Kar, T.; Scheiner, S. *J. Am. Chem. Soc.* **1999**, *121*, 9411.
(50) The CH_2 peaks from the butyl chain did not shift much with concentration change and held fixed in fitting the spectra.
(51) Saha, S.; Hamaguchi, H. *J. Phys. Chem. B* **2006**, *110*, 2777.
(52) Li, W.; Zhang, Z.; Han, B.; Hu, S.; Xie, Y.; Yang, G. *J. Phys. Chem. B* **2007**, *111*, 6452.
(53) Max, J.-J.; Chapados, C. *J. Chem. Phys.* **2003**, *119*, 5632.